SUPPORTING INFORMATION FOR

Parallel screening for rapid identification of orthogonal bioluminescent tools

Colin M. Rathbun[#,1], William B. Porterfield[#,1], Krysten A. Jones[#,2], Marian J. Sagoe[1], Monique R. Reyes[3], Christine T. Hua[2], and Jennifer A. Prescher*[1-3]

[1]Departments of Chemistry, [2]Molecular Biology & Biochemistry, and [3]Pharmaceutical Sciences, University of California Irvine, CA 92697, USA
[#] These authors contributed equally
* Correspondence should be addressed to
J.A.P. (jpresche@uci.edu)
949-824-1706

TABLE OF CONTENTS

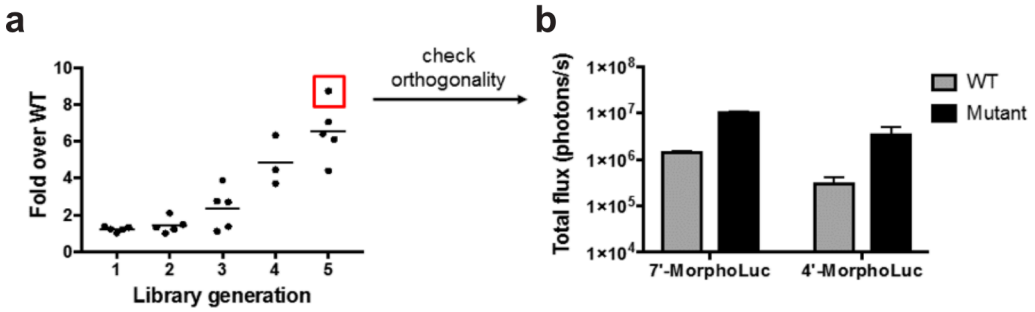

Figure S1. "Brighter" mutants can be evolved but are not orthogonal. (a) Fold increase in light emission tracked over five generations. Mutants were screened for total photon output with 7′–MorphoLuc. (b) The brightest mutant (red box in (a)) with 7′–MorphoLuc also exhibited increased photon output with 4′–MorphoLuc (black bars). Photon flux values for native Fluc (gray bars) are also shown. Imaging was performed in bacterial lysate (250 μM luciferin analogue).

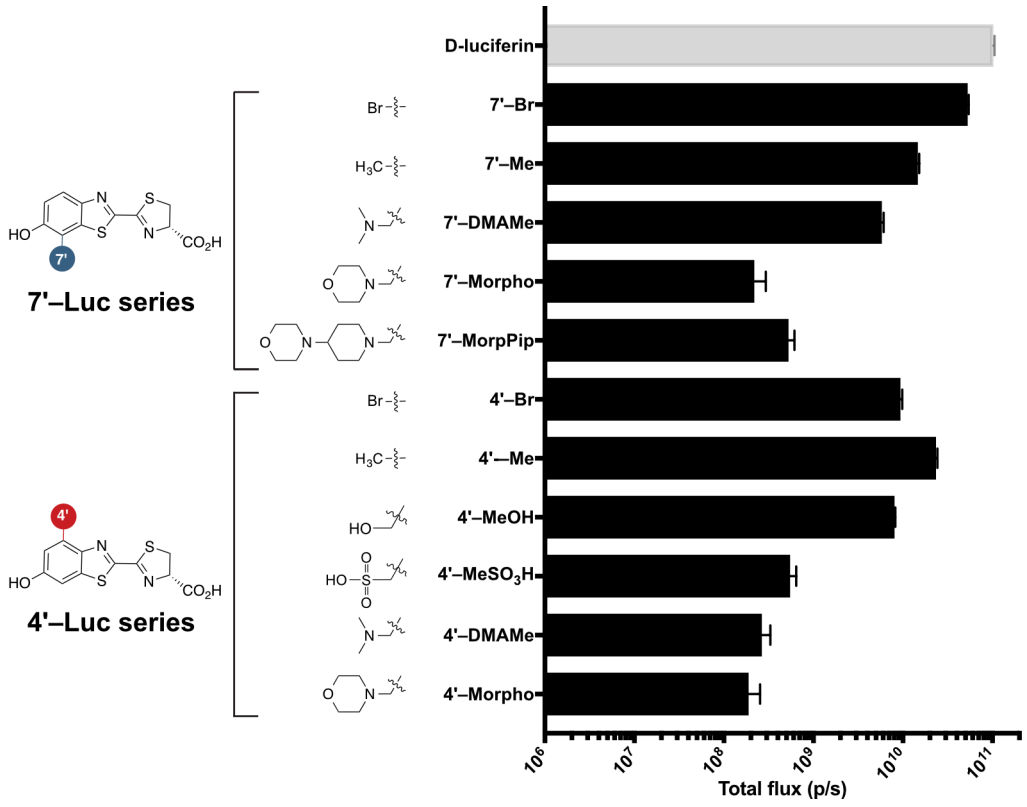

Figure S2. Sterically modified luciferins emit varying levels of photons with Fluc. Fluc (1 μg) was incubated with 100 μM luciferin analogue and photon outputs were measured. Error bars represent the standard error of the mean for n ≥ 3 independent experiments.

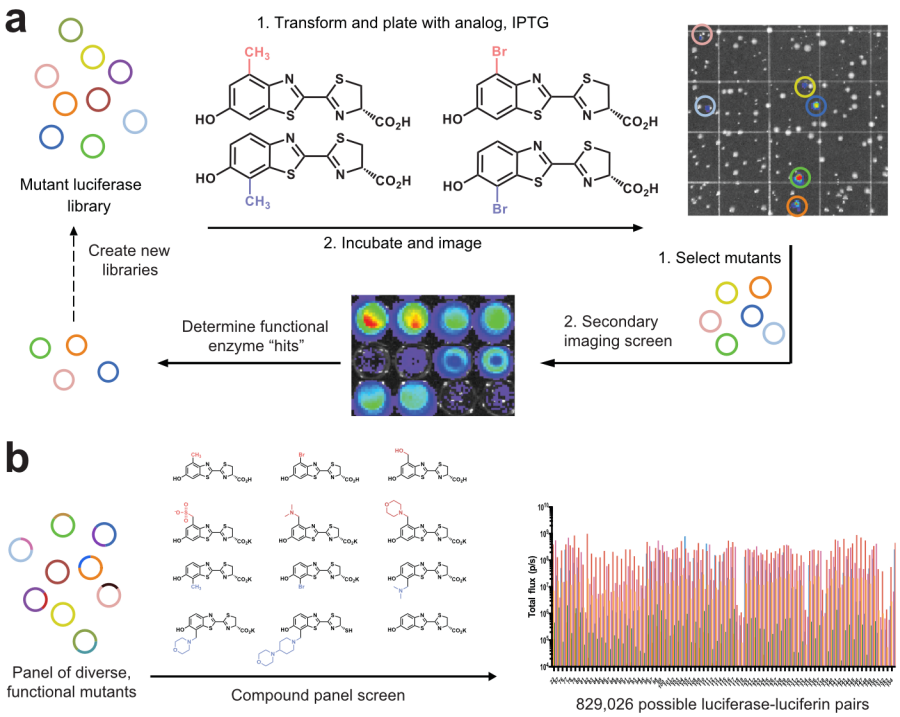

Figure S3. Screening for orthogonal pairs among enriched, functional luciferases. (a) Mutant luciferase libraries were generated and screened on-plate with minimally perturbed luciferins. Functional mutants were identified and analyzed by a secondary screen to determine "hits". Some "hits" were pooled and subjected to further mutagenesis for additional screening. (b) A panel of 159 functionally diverse mutants (identified from (a)) was incubated with 12 luciferin analogues (in lysate) and imaged, generating 1908 individual data points. (A subset of light emission data is shown in the bar graph.) From this collection, 829,026 luciferase-luciferin pairs were possible.

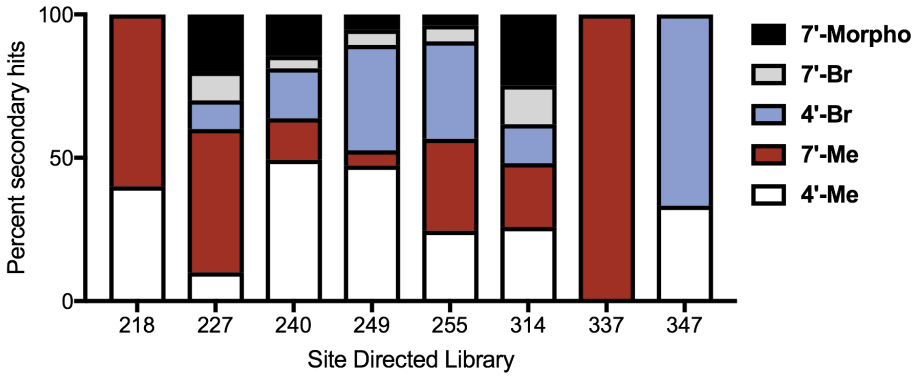

Figure S4. Distribution of "hits" identified from on-plate screens. Unique luciferases were identified from screens with minimally perturbed luciferin analogues.

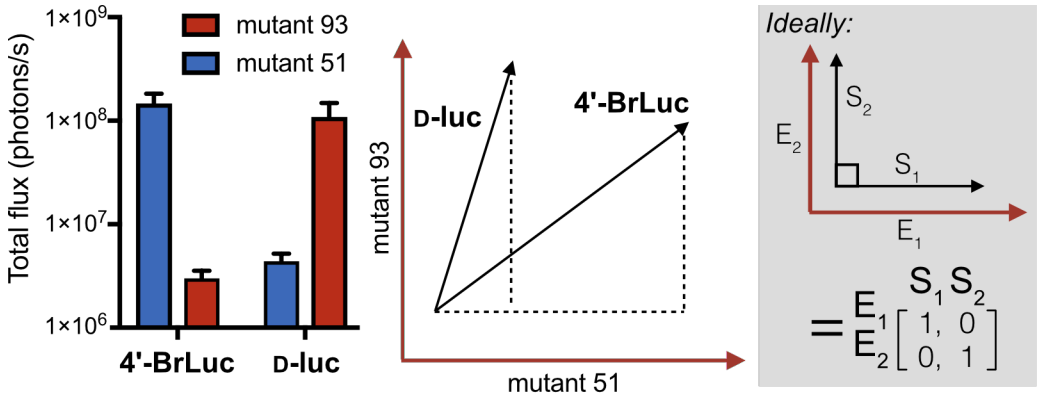

Figure S5. Vector analysis of light emission data. Imaging data with luciferase-luciferin pairs can be represented by vector units. Sample data with two mutants and analogues are shown. Perfect orthogonality is defined as the identity matrix.

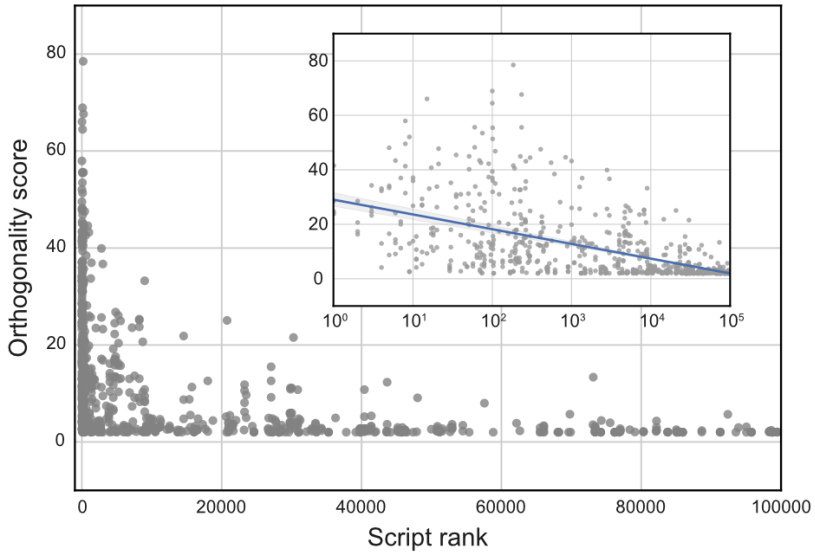

Figure S6. Biochemical verification of orthogonal pairs predicted from computer script. Each point compares the experimentally measured orthogonality score for a given pair with its rank predicted by the computer algorithm. (The inset shows the data plotted on a logarithmic scale). A clear positive relationship is observed; as the ranking increases, so does the observed orthogonality.

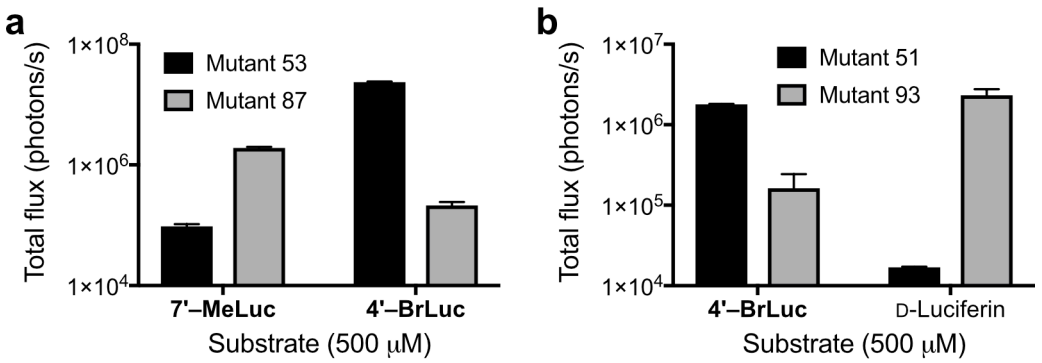

Figure S7. Multicellular imaging with orthogonal pairs. Lead pairings of (a) mutants 53 and 87 and (b) 51 and 93 maintain orthogonality in mammalian cell culture. In each case, 100,000 DB7 cells were treated with 500 μM luciferin analogue and imaged. Error bars represent SEM for experiments performed in triplicate.

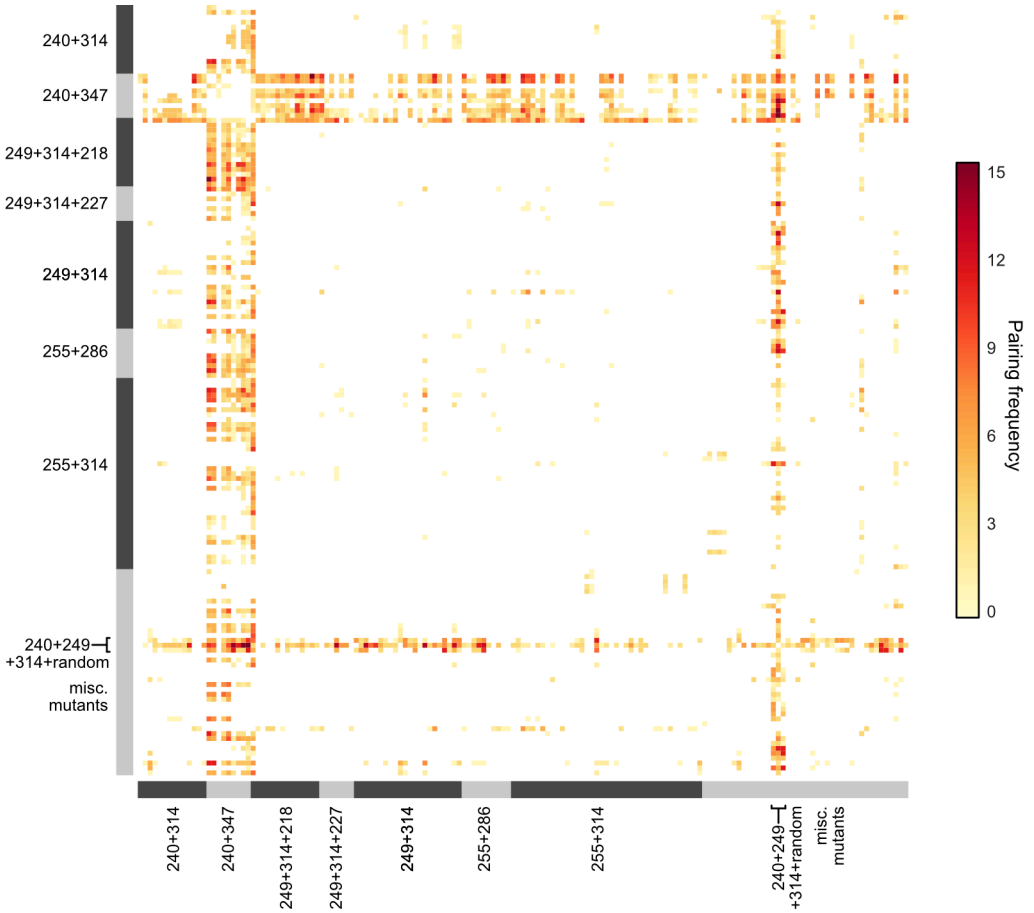

Figure S8. Origins of mutant enzymes that comprise orthogonal pairs. The top 5,000 *in silico* hits are shown, with each square representing an orthogonal pair. Each axis denotes Fluc residues targeted for mutagenesis. Mutants are grouped along each axis corresponding to their library of origin.

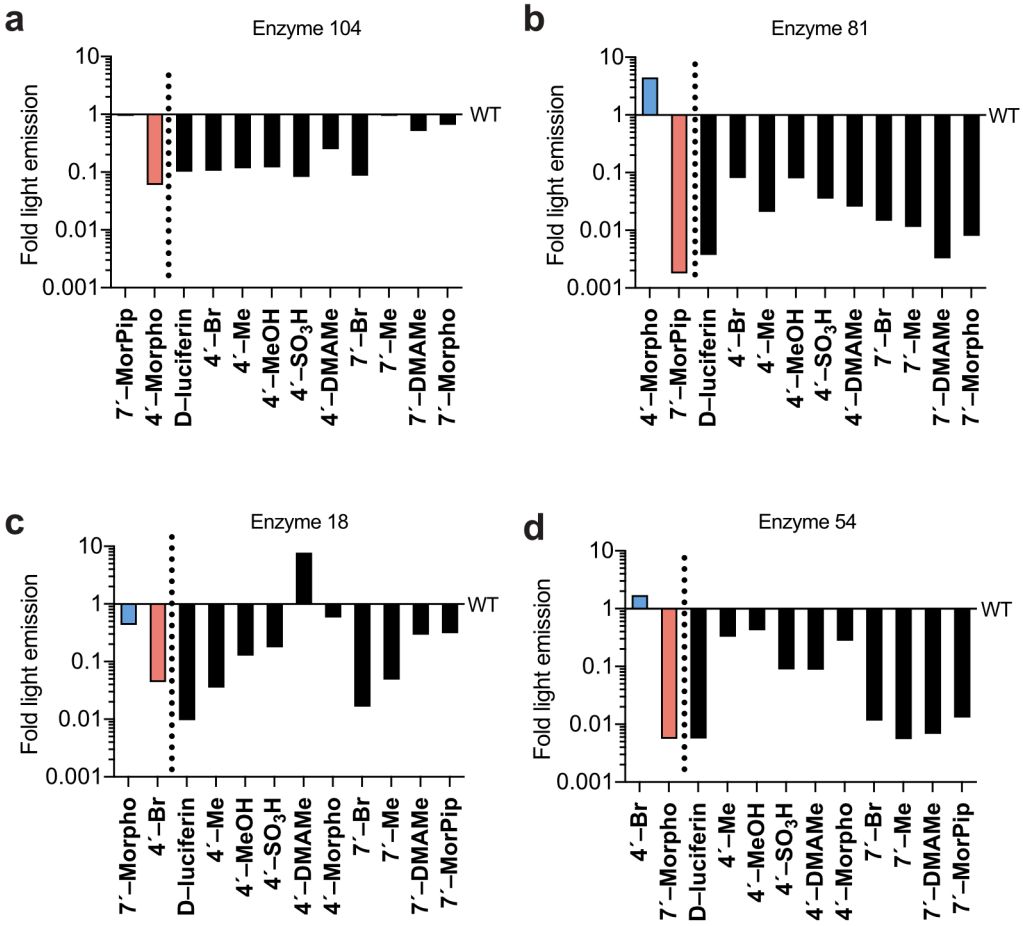

Figure S9. Selectivities of mutant enzymes for synthetic luciferins. Lead orthogonal enzymes (a) 104, (b) 81, (c) 18, and (d) 54 were treated with a panel of luciferin analogues and imaged. Light emission values are plotted as fold changes from Fluc with the respective compound (for normalization). The positive (blue) and negative (red) pairs are shown on the left side in each case.

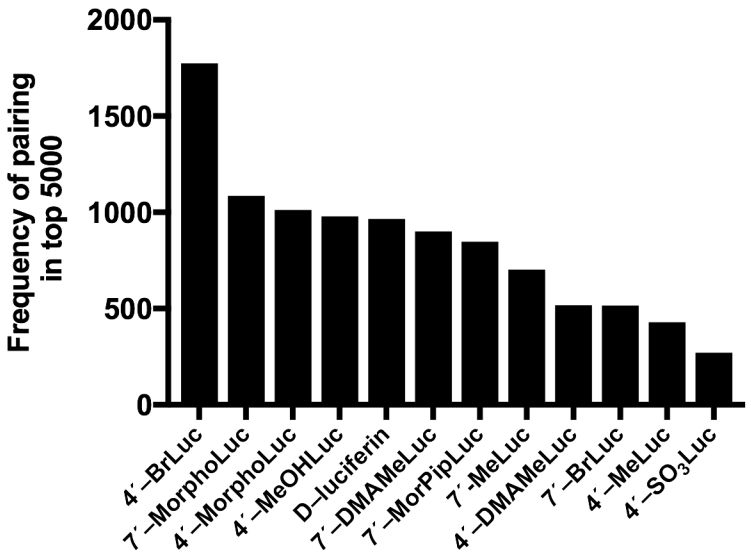

Figure S10. Propensity for orthogonality. Frequency of compounds appearing in the top 0.6% (5,000 out of 829,000) of orthogonal pairs.

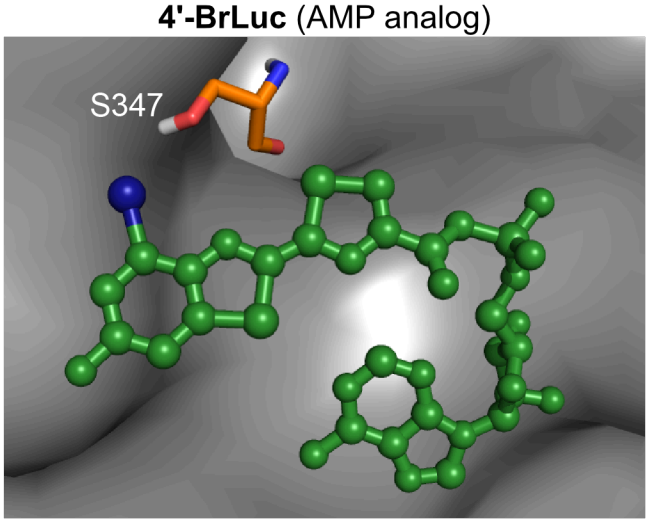

Figure S11. AutoDock analysis with 4´–BrLuc in native Fluc. Potential steric clash revealed between bromo substituent (blue) on 4´-BrLuc (shown as AMP conjugate, green) and S347 in Fluc. This residue is mutated to Gly in enzymes 51 and 53, which process the analogue. PDB:4G36.

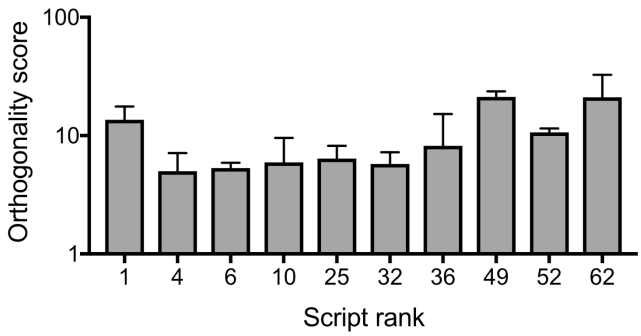

Figure S12. "Triplet" imaging with orthogonal pairs. Unique sets of three luciferase-luciferin pairs were identified. The top 10 unique triplet sets predicted *in silico* were verified *in vitro*. Bacteria expressing mutant enzymes were expanded, lysed and imaged with substrate. Orthogonality scores were measured as above. Error bars represent the standard error of the mean for n = 3 experiments.

Table S1. List of mutant luciferases.

Mutant number	Name	Sequence
1	4Me lead	F227C, M249L, S314T, A348G
2	7Br3C lead	R218H, F250T, S314C, Q338C
3	7Br3L lead	R218H, F250T, S314C, Q338L
4	7Br4C lead	R218H, F250T, S314C, G316T, Q338C
5	7Br4V lead	R218H, F250T, S314C, G316T, Q338V
13	G3_7Mor_16	M249F, T252S, F295L, S314T, G316T, A326V, P334S
14	G3_7Mor_18	M249L, S314V, G316S
15	G3_7Mor_21	M249L, S314C, G316A
16	G3_7Mor_24	M249F, Y266H, S293N, S314C, G316A
17	G3_7Mor_3	M249F, F294S, S314T, G316T
18	G3_7Mor_36	V240A, M249L, M265T, F295L, I301T, S314T, G316T, L321R
19	G3_7Mor_4	M249L, F294L, D305E, S314T, G316T
20	G3_7Mor_46	M249L, L267F, S314T, G316T
21	G3_7Mor_5	M249F, S314T, G316T
22	G3_7Mor_57	M249F, Y266H, L295F, I312V
23	G3_7Mor_58	V240A, M249L, L264F, S314T, G316T, K321R
24	G3_7Mor_65	M249L, Q283R, S314T, G316T
25	G3_7Mor_76	I226V, V240A, M249L, I282T, F295L, S314T, G316T
26	G3_7Mor_86	I226V, M249F, D279N, S314T, G316T
27	G3_7Mor_88	I232T, M249L, S314T, G316T
28	G3_7Mor_89	M249F, I282V, H310R, S314T, G316T
29	G5_7Mor_14	F227W, M249L, L286M, L287V, V288M, S314T, G316T
30	G5_7Mor_4	F227W, M249L, L287V, V288M, S314T, G316T
31	G5_7Mor_5	F227W, M249L, L287V, V288L, S314T, G316T
32	G5_7Mor_7	F227W, M249L, V288L, S314T, G316T

Mutant number	Name	Sequence
33	G5_7Mor_8	F227Y, M249L, L286M, L287V, V288L, S314T, G316T
34	WT	WT
35	R218A	R218A
36	R218H	R218H
37	R218K	R218K
38	rand_4Mor_28	T214A, E269G
39	rand_4Mor_31	K281E, F295L
40	rand_4Mor_38	T290A, F294S
41	rand_4Mor_60	I312V
42	rand_4Mor_71	H310R
43	rand_4Mor_83	E269G
44	SD240+314_7Me_11	V240I, V241A, S314T
45	SD240+314_7Me_13	V240A, V241A, F247L, S314T
47	SD240+314_7Me_21	V240A, F243M, S314T
48	SD240+314_7Me_32	F243M, S314T
49	SD240+314_7Me_40	V240A, F247Y, S314T
50	SD240+347_4Br_1	V240I, F247Y, S347G
51	SD240+347_4Br_12	F243M, S347G
52	SD240+347_4Br_17	V240A, V241M, F243M, F247Y
53	SD240+347_4Br_6	V240I, F243M, F247Y, S347G
54	SD240+347_4Me_14	V241A, F247L, S347A
55	SD240+347_4Me_3	V240L, V241L, F247Y, S347A
56	SD240+347_4Me_36	V240M, F243M, F247Y, S347A
57	SD240+347_4Me_39	V240G, F247Y, S347A
58	SD240+347_4Me_9	F243M, F247Y, S347A
59	SD249+314_4Br_14	S314C, G316T
60	SD249+314_4Br_15	S314T
61	SD249+314_4Br_16	M249L, S314C, G316S
62	SD249+314_4Br_18	M249L, F250M, S314C
63	SD249+314_4Br_22	M249L, S314C, G316A
64	SD249+314_4Br_3	S314C, G316S
65	SD249+314_4Br_38	M249L, G316S
66	SD249+314_4Br_43	M249F, S314C, G316S
67	SD249+314_4Me_16	F250Y, S314
68	SD249+314_4Me_2	F250M, S314T, G316T
69	SD249+314_4Me_21	F250Y, S314T, G316T
70	SD249+314_4Me_24	M249L, S314C
71	SD249+314_4Me_47	S314C, G316A
72	SD249+314_4Me_5	S314A, G316S
73	SD249+314_4Me_51	F250T, S314T, G316T
74	SD249+314_7Br_24	F250H, S314C
75	SD249+314_7Br_3	F250T, S314C
76	SD249+314_7Br_4	F250T, S314C, G316T
77	SD249+314_7Me_21	M249L, S314T
78	SD249+314_7Me_25	M249L, S314V
79	SD249+314_7Me_4	M249L, S314T, G316S

Mutant number	Name	Sequence
80	SD249+314_7Me_5	M249L, S314T, G316T
81	SD249+314+218_4Me_1	R218A, F250M, S314T, G316T
82	SD249+314+218_4Me_13	R218K, F250M, S314T, G316T
83	SD249+314+218_4Me_15	R218K, S314C, G316A
85	SD249+314+218_4Me_25	R218K, F250M, S314T, G316T
86	SD249+314+218_4Me_27	R218K, M249L, S314C
87	SD249+314+218_4Me_34	R218K, F250Y, S314T, G316T
88	SD249+314+218_4Me_35	R218K, F250M, S314C
89	SD249+314+218_4Me_5	R218K, S314T, G316T
90	SD249+314+218_4Me_9	R218K, F250Y, S314C
91	SD249+314+218_7Me_2	R218K, M249L, S314T
92	SD249+314+218_7Me_24	R218K, M249L, S314T, G316S
93	SD249+314+218_7Me_27	R218K, M249L, S314V
94	SD249+314+218_7Me_30	R218K, M249L, S314V, G316S
95	SD249+314+227_4Br_1	F227Y, M249L, F250Y, G316S
96	SD249+314+227_4Br_2	F227Y, M249L, S314C
97	SD249+314+227_4Br_3	F227Y, S314C, G316T
98	SD249+314+227_4Br_5	F227Y, S314T
99	SD249+314+227_4Br_6	F227Y, S314C, G316A
100	SD249+314+227_4Br_8	F227Y, M249L, S314C, G316S
101	SD249+314+227_7Br_1	F227Y, F250H, S314C
102	SD255+314_4Br_10	Y255F, L256I, I257V, S314C
103	SD255+314_4Br_11	Y255H, I257V, S314C
104	SD255+314_4Br_2	L256I, I257F, S314T
105	SD255+314_4Br_27	L256I, I257F, S314C, G316S
107	SD255+314_4Br_40	Y255N, I257V, S314C, G316T
108	SD255+314_4Br_42	Y255H, I257V, S314C
109	SD255+314_4Br_49	Y255N, I257V, S314C
110	SD255+314_4Br_5	S347A
111	SD255+314_4Br_50	L256I, I257F, S314C, G316T
112	SD255+314_4Br_59	not sequenced
113	SD255+314_4Br_61	Y255H, I257V, G316S
114	SD255+314_4Br_62	Y255F, L256I, I257V, S314C, G316S
115	SD255+314_4Br_64	L256M, I257C, S314C
116	SD255+314_4Br_9	Y255F, I257L, S314T
117	SD255+314_4Me_1	I257M, S314T
118	SD255+314_4Me_10-1	I257S, 314V, G315H, G316R
119	SD255+314_4Me_10-3	Y255H, S314V
120	SD255+314_4Me_13	I257A, S314C
121	SD255+314_4Me_18	I257C, S314T, G316T
122	SD255+314_4Me_6	L256M, S314V, G316S
123	SD255+314_4Me_7	I257S, S314T, G316T
124	SD255+314_7Br_10	Y255F, I257L, S314C, G316T
125	SD255+314_7Br_15	Y255F, I257L, S314V, G316T
126	SD255+314_7Br_3	Y255F, I257L, S314C, G316A
127	SD255+314_7Br_5	Y255F, I257L, S314C, G316S

Mutant number	Name	Sequence
128	SD255+314_7Br_6	Y255F, I257L, S314V, G316S
129	SD255+314_7Br_8	Y255F, I257L, S314C
130	SD255+314_7Me_14	I257R, S314T, G316S
131	SD255+314_7Me_21	Y255H, I257R, S314C, G316A
132	SD255+314_7Me_22	Y255H, I257S, S314V
133	SD255+314_7Me_25	Y255F, I257L, G316S
134	SD255+314_7Me_27	not sequenced
135	SD255+314_7Me_29	Y255F, I257M, S314C, G316A
136	SD255+314_7Me_31	Y255H, I257L, S314T, G316T
137	SD255+314_7Me_35	Y255F, I257M, S314V, G316S
138	SD255+314_7Me_36	Y255F, I257L, S314A, G316S
139	SD255+314_7Me_37	Y255F, I257L, G316A
140	SD255+314_7Me_48	Y255H, I257R, S314T, G316S
141	SD255+314_7Me_8	L256M, I257F, S314T, G316T
142	SD240+314_4Br_1	V240L, V241F, F247S, S314C, G316A
143	SD240+314_4Br_8	V240A, V241A, S314C, G316S
144	SD240+314_4Me_1	V241A, F247Y, S314T, G316T
145	SD240+314_4Me_6	V241A, F243L, F247Y, S314C
146	SD240+314_4Me_15	V241A, F247L, S314T, G316T
147	SD240+314_7Me_2	V240M, V241M, F247Y, S314V
148	SD240+314_7Me_5	V240A, V241A, F247L, S314C, G316A
149	SD240+314_7Me_13	F243M, G316S
150	SD240+314_7Me_16	F243M
156	SD255+286_4Me113	Y255H, L286V, L287M, V288A
157	SD255+286_4Me143	L256I, I257M, L286V, V288A
158	SD255+286_7Me30	L256M, I257F, L286I, L287V, V288L
159	SD255+286_7Me31	Y255I, I257C, L287V, V288A

Materials and methods

General bioluminescence imaging

All analyses were performed in black 96-well plates (Greiner Bio One). Plates containing luminescent reagents were imaged in a light-proof chamber with an IVIS Lumina (Xenogen) CCD camera chilled to -90 ºC. The stage was kept at 37 ºC during the imaging session, and the camera was controlled using Living Image software. Exposure times ranged from 1 s to 5 min, with data binning levels set to small or medium. Regions of interest were selected for quantification and total flux values were analyzed using Living Image software.

Construction of luciferase libraries

Two sections of the luciferase gene (*pgl4-luc2*), denoted R1 and R2, were targeted for gene assembly as described in Jones *et al.*[1] To assemble mutant libraries, primers containing the codon(s) of interest (Supplementary Tables 2-9) were used in place of the primer coding for the wild-type sequence. Other libraries were created using standard QuikChange PCR techniques (Supplementary Table 10). All PCR reactions were run using Q5 Hot-start DNA polymerase (New England BioLabs).

Libraries were inserted into linearized template vectors pET28-R1del or pET28-R2del as described in Jones *et al.*[1] Library inserts were assembled with linearized pET vectors using circular polymerase extension cloning (CPEC) as described in Jones *et al.*[1] or by Gibson assembly. Gibson assembly master mixes were prepared following the Prather recipe on http://www.openwetware.org/wiki/Gibson_Assembly, with all materials purchased from New England BioLabs. For each assembly, 50 ng of *Dpn*I digested, linearized vector was combined with insert (2:1 to 8:1 insert:vector rations) and added to 10 µL of master mix. The mixtures were incubated at 50 °C for 20-60 min, then 1-3 µL was transformed into chemically competent cells (Top10 or DH5α *E. coli*). Transformants were plated on square, agar plates containing kanamycin. Cells were plated to exceed 3X the library size. Cells were scraped off of the plates, combined, and pelleted. DNA was isolated via miniprep and saved for agar-plate screening.

Supplementary Tables 2-10: Primers used to construct site-directed (SD) libraries. The bases highlighted in red denote sites targeted for saturation mutagenesis.

Supplementary Table 2: SD218 primers	
Forward primers	
SD218-F1	GCACCGCACCGCTTGTGTCKGGTTCAGTCATGCCC
SD218-F2	GCACCGCACCGCTTGTGTCWKTTTCAGTCATGCCC
SD218-F3	GCACCGCACCGCTTGTGTCVHGTTCAGTCATGCCC
SD218-F4	GCACCGCACCGCTTGTGTCNATTTCAGTCATGCCC
Reverse primers	
SD218-R1	GCCGAAGATGGGGTCGCGGGCATGACTGAACCMGAC
SD218-R2	GCCGAAGATGGGGTCGCGGGCATGACTGAAAMWGAC
SD218-R3	GCCGAAGATGGGGTCGCGGGCATGACTGAACDBGAC
SD218-R4	GCCGAAGATGGGGTCGCGGGCATGACTGAAATNGAC

Supplementary Table 3: SD227 primers	
Forward primers	
SD227-F1	GCGACCCCATCTGKGGCAACCAGATCATCCCCGACA
SD227-F2	GCGACCCCATCVBCGGCAACCAGATCATCCCCGACA
SD227-F3	GCGACCCCATCATGGGCAACCAGATCATCCCCGACA
SD227-F4	GCGACCCCATCNAWGGCAACCAGATCATCCCCGACA
Reverse primers	
SD227-R1	GCCMCAGATGGGGTCGCGGGCATGACTGAATCGGAC
SD227-R2	GCCGVBGATGGGGTCGCGGGCATGACTGAATCGGAC
SD227-R3	GCCCATGATGGGGTCGCGGGCATGACTGAATCGGAC
SD227-R4	GCCWTNGATGGGGTCGCGGGCATGACTGAATCGGAC

Supplementary Table 4: SD240 primers	
Forward primers	
SD240-F1	CCGCTATCCTCAGCGBCGBCCCAGBCCACCACGGC
SD240-F2	CCGCTATCCTCAGCGBCGBCCCAWTKCACCACGGC
SD240-F3	CCGCTATCCTCAGCGBCWTKCCAGBCCACCACGGC
SD240-F4	CCGCTATCCTCAGCWTKGBCCCAGBCCACCACGGC
SD240-F5	CCGCTATCCTCAGCWTKWTKCCAGBCCACCACGGC
SD240-F6	CCGCTATCCTCAGCWTKGBCCCAWTKCACCACGGC
SD240-F7	CCGCTATCCTCAGCGBCWTKCCAWTKCACCACGGC
SD240-F8	CCGCTATCCTCAGCWTKWTKCCAWTKCACCACGGC
SD240-F9	NDTGGCATGTTCACCACGCTGGGCTACTTGATCTGCG
SD240-F10	VHGGGCATGTTCACCACGCTGGGCTACTTGATCTGCG
SD240-F11	TGGGGCATGTTCACCACGCTGGGCTACTTGATCTGCG
Reverse primers	
SD240-R1	GVCGVCGCTGAGGATAGCGGTGTCGGGGATGATCTGGTT
SD240-R2	MAWMAWGCTGAGGATAGCGGTGTCGGGGATGATCTGGTT
SD240-R3	MAWGVCGCTGAGGATAGCGGTGTCGGGGATGATCTGGTT
SD240-R4	GVCMAWGCTGAGGATAGCGGTGTCGGGGATGATCTGGTT
SD240-R5	CGTGGTGAACATGCCAHNGCCGTGGTGGVCTGG
SD240-R6	CGTGGTGAACATGCCCDBGCCGTGGTGGVCTGG
SD240-R7	CGTGGTGAACATGCCCCAGCCGTGGTGGVCTGG

SD240-R8	CGTGGTGAACATGCCAHNGCCGTGGTGMAWTGG
SD240-R9	CGTGGTGAACATGCCCDBGCCGTGGTGMAWTGG
SD240-R10	CGTGGTGAACATGCCCCAGCCGTGGTGMAWTGG

Supplementary Table 5: SD249 primers	
Forward primers	
SD249-F1	CACGGCTTCGGCGBCNDTNDTACGCTGGGCTACTTGATCTGCGG
SD249-F2	CACGGCTTCGGCGBCNDTVHGACGCTGGGCTACTTGATCTGCGG
SD249-F3	CACGGCTTCGGCGBCNDTTGGACGCTGGGCTACTTGATCTGCGG
SD249-F4	CACGGCTTCGGCGBCVHGNDTACGCTGGGCTACTTGATCTGCGG
SD249-F5	CACGGCTTCGGCGBCVHGVHGACGCTGGGCTACTTGATCTGCGG
SD249-F6	CACGGCTTCGGCGBCVHGTGGACGCTGGGCTACTTGATCTGCGG
SD249-F7	CACGGCTTCGGCGBCTGGNDTACGCTGGGCTACTTGATCTGCGG
SD249-F8	CACGGCTTCGGCGBCTGGVHGACGCTGGGCTACTTGATCTGCGG
SD249-F9	CACGGCTTCGGCGBCTGGTGGACGCTGGGCTACTTGATCTGCGG
SD249-F10	CACGGCTTCGGCWTKNDTNDTACGCTGGGCTACTTGATCTGCGG
SD249-F11	CACGGCTTCGGCWTKNDTVHGACGCTGGGCTACTTGATCTGCGG
SD249-F12	CACGGCTTCGGCWTKNDTTGGACGCTGGGCTACTTGATCTGCGG
SD249-F13	CACGGCTTCGGCWTKVHGNDTACGCTGGGCTACTTGATCTGCGG
SD249-F14	CACGGCTTCGGCWTKVHGVHGACGCTGGGCTACTTGATCTGCGG
SD249-F15	CACGGCTTCGGCWTKVHGTGGACGCTGGGCTACTTGATCTGCGG
SD249-F16	CACGGCTTCGGCWTKTGGNDTACGCTGGGCTACTTGATCTGCGG
SD249-F17	CACGGCTTCGGCWTKTGGVHGACGCTGGGCTACTTGATCTGCGG
SD249-F18	CACGGCTTCGGCWTKTGGTGGACGCTGGGCTACTTGATCTGCGG
Reverse primers	

SD249-R1	GVCAHNAHNGCCGAAGCCGTGGTGAAATGG
SD249-R2	GVCAHNCDBGCCGAAGCCGTGGTGAAATGG
SD249-R3	GVCAHNCCAGCCGAAGCCGTGGTGAAATGG
SD249-R4	GVCCDBAHNGCCGAAGCCGTGGTGAAATGG
SD249-R5	GVCCDBCDBGCCGAAGCCGTGGTGAAATGG
SD249-R6	GVCCDBCCAGCCGAAGCCGTGGTGAAATGG
SD249-R7	GVCCCAAHNGCCGAAGCCGTGGTGAAATGG
SD249-R8	GVCCCACDBGCCGAAGCCGTGGTGAAATGG
SD249-R9	GVCCCACCAGCCGAAGCCGTGGTGAAATGG
SD249-R10	MAWAHNNDTGCCGAAGCCGTGGTGAAATGG
SD249-R11	MAWAHNCDBGCCGAAGCCGTGGTGAAATGG
SD249-R12	MAWAHNCCAGCCGAAGCCGTGGTGAAATGG
SD249-R13	MAWCDBAHNGCCGAAGCCGTGGTGAAATGG
SD249-R14	MAWCDBCDBGCCGAAGCCGTGGTGAAATGG
SD249-R15	MAWCDBCCAGCCGAAGCCGTGGTGAAATGG
SD249-R16	MAWCCAAHNGCCGAAGCCGTGGTGAAATGG
SD249-R17	MAWCCACDBGCCGAAGCCGTGGTGAAATGG
SD249-R18	MAWCCACCAGCCGAAGCCGTGGTGAAATGG

Supplementary Table 6: SD255 primers	
Forward primers	
SD255-F1	TTCGGCATGTTCACCACGCTGGGCNDTNDTNDTTGCG
SD255-F2	TTCGGCATGTTCACCACGCTGGGCNDTNDTVHGTGCG
SD255-F3	TTCGGCATGTTCACCACGCTGGGCNDTNDTTGGTGCG
SD255-F4	TTCGGCATGTTCACCACGCTGGGCNDTVHGNDTTGCG
SD255-F5	TTCGGCATGTTCACCACGCTGGGCNDTVHGVHGTGCG
SD255-F6	TTCGGCATGTTCACCACGCTGGGCNDTVHGTGGTGCG
SD255-F7	TTCGGCATGTTCACCACGCTGGGCNDTTGGNDTTGCG
SD255-F8	TTCGGCATGTTCACCACGCTGGGCNDTTGGVHGTGCG
SD255-F9	TTCGGCATGTTCACCACGCTGGGCNDTTGGTGGTGCG
Reverse primers	
SD255-R1	AGCACGACCCGAAAGCCGCAAHNAHNAHNGCCCAG
SD255-R2	AGCACGACCCGAAAGCCGCACDBAHNAHNGCCCAG
SD255-R3	AGCACGACCCGAAAGCCGCACCAAHNAHNGCCCAG
SD255-R4	AGCACGACCCGAAAGCCGCAAHNCDBAHNGCCCAG
SD255-R5	AGCACGACCCGAAAGCCGCACDBCDBAHNGCCCAG
SD255-R6	AGCACGACCCGAAAGCCGCACCACDBAHNGCCCAG
SD255-R7	AGCACGACCCGAAAGCCGCAAHNCCAAHNGCCCAG
SD255-R8	AGCACGACCCGAAAGCCGCACDBCCAAHNGCCCAG
SD255-R9	AGCACGACCCGAAAGCCGCACCACCAAHNGCCCAG

Supplementary Table 7: SD286 primers	
Forward primers	
SD286-F1	AGACTATAAGATTCAATCTGCCGBCGBCGBCCCCACAC
SD286-F2	AGACTATAAGATTCAATCTGCCGBCWTKWTKCCCACAC
SD286-F3	AGACTATAAGATTCAATCTGCCGBCWTKGBCCCCACAC
SD286-F4	AGACTATAAGATTCAATCTGCCGBCGBCWTKCCCACAC
SD286-F5	AGACTATAAGATTCAATCTGCCWTKWTKWTKCCCACAC
SD286-F6	AGACTATAAGATTCAATCTGCCWTKGBCGBCCCCACAC
SD286-F7	AGACTATAAGATTCAATCTGCCWTKGBCWTKCCCACAC
SD286-F8	AGACTATAAGATTCAATCTGCCWTKWTKGBCCCCACAC
Reverse primers	
SD286-R1	GCTCTTAGCGAAGAAGCTAAATAGTGTGGGGVCGVCGVC
SD286-R2	GCTCTTAGCGAAGAAGCTAAATAGTGTGGGMAWMAWGVC
SD286-R3	GCTCTTAGCGAAGAAGCTAAATAGTGTGGGGVCMAWGVC
SD286-R4	GCTCTTAGCGAAGAAGCTAAATAGTGTGGGMAWGVCGVC
SD286-R5	GCTCTTAGCGAAGAAGCTAAATAGTGTGGGMAWMAWMAW
SD286-R6	GCTCTTAGCGAAGAAGCTAAATAGTGTGGGGVCGVCMAW
SD286-R7	GCTCTTAGCGAAGAAGCTAAATAGTGTGGGMAWGVCMAW
SD286-R8	GCTCTTAGCGAAGAAGCTAAATAGTGTGGGGVCMAWMAW

Supplementary Table 8: SD314 primers	
Forward primers	
SD314-F1	CTAAGCAACTTGCACGAGATCGCCNDTNDTNDT
SD314-F2	CTAAGCAACTTGCACGAGATCGCCNDTNDTVHG
SD314-F3	CTAAGCAACTTGCACGAGATCGCCNDTNDTTGG
SD314-F4	CTAAGCAACTTGCACGAGATCGCCVHGNDTNDT
SD314-F5	CTAAGCAACTTGCACGAGATCGCCVHGNDTVHG
SD314-F6	CTAAGCAACTTGCACGAGATCGCCVHGNDTTGG
SD314-F7	CTAAGCAACTTGCACGAGATCGCCTGGNDTNDT
SD314-F8	CTAAGCAACTTGCACGAGATCGCCTGGNDTVHG

SD314-F9	CTAAGCAACTTGCACGAGATCGCCTGGNDTTGG
Reverse primers	
SD314-R1	TTGCTGAGCGGCGCAHNAHNAHNGGCGATC
SD314-R2	TTGCTGAGCGGCGCCDBAHNAHNGGCGATC
SD314-R3	TTGCTGAGCGGCGCCCAAHNAHNGGCGATC
SD314-R4	TTGCTGAGCGGCGCAHNAHNCDBGGCGATC
SD314-R5	TTGCTGAGCGGCGCCDBAHNCDBGGCGATC
SD314-R6	TTGCTGAGCGGCGCCCAAHNCDBGGCGATC
SD314-R7	TTGCTGAGCGGCGCAHNAHNCCAGGCGATC
SD314-R8	TTGCTGAGCGGCGCCDBAHNCCAGGCGATC
SD314-R9	TTGCTGAGCGGCGCCCAAHNCCAGGCGATC

Supplementary Table 9: SD337 primers	
Forward primers	
SD337-F1	NDTNDTGGCNDTGGCCTGACAGAAACAACTAGTGCCA
SD337-F2	NDTVHGGGCNDTGGCCTGACAGAAACAACTAGTGCCA
SD337-F3	NDTTGGGGCNDTGGCCTGACAGAAACAACTAGTGCCA
SD337-F4	VHGNDTGGCNDTGGCCTGACAGAAACAACTAGTGCCA
SD337-F5	VHGVHGGGCNDTGGCCTGACAGAAACAACTAGTGCCA
SD337-F6	VHGTGGGGCNDTGGCCTGACAGAAACAACTAGTGCCA
SD337-F7	TGGNDTGGCNDTGGCCTGACAGAAACAACTAGTGCCA
SD337-F8	TGGVHGGGCNDTGGCCTGACAGAAACAACTAGTGCCA
SD337-F9	TGGTGGGGCNDTGGCCTGACAGAAACAACTAGTGCCA
Reverse primers	
SD337-R1	AGGCCAHNGCCAHNAHNGATGCCTGGTAGGT
SD337-R2	AGGCCAHNGCCAHNCDBGATGCCTGGTAGGT
SD337-R3	AGGCCAHNGCCAHNCCAGATGCCTGGTAGGT
SD337-R4	AGGCCAHNGCCCDBAHNGATGCCTGGTAGGT
SD337-R5	AGGCCAHNGCCCDBCDBGATGCCTGGTAGGT
SD337-R6	AGGCCAHNGCCCDBCCAGATGCCTGGTAGGT
SD337-R7	AGGCCAHNGCCCCAAHNGATGCCTGGTAGGT
SD337-R8	AGGCCAHNGCCCCACDBGATGCCTGGTAGGT
SD337-R9	AGGCCAHNGCCCCACCAGATGCCTGGTAGGT

Supplementary Table 10: SD347 primers	
Reverse primers	
SD347-R1	CTTCGGGGGTGATCAGAATAHNAHNAGTTGTTTCTGTC AGGCCG
SD347-R2	CTTCGGGGGTGATCAGAATAHNCDBAGTTGTTTCTGTCA

	GGCCG
SD347-R3	CTTCGGGGGTGATCAGAATAHNCCAAGTTGTTTCTGTCA GGCCG
SD347-R4	CTTCGGGGGTGATCAGAATCDBAHNAGTTGTTTCTGTCA GGCCG
SD347-R5	CTTCGGGGGTGATCAGAATCDBCDBAGTTGTTTCTGTCA GGCCG
SD347-R6	CTTCGGGGGTGATCAGAATCDBCCAAGTTGTTTCTGTCA GGCCG
SD347-R7	CTTCGGGGGTGATCAGAATCCAAHNAGTTGTTTCTGTCA GGCCG
SD347-R8	CTTCGGGGGTGATCAGAATCCACDBAGTTGTTTCTGTCA GGCCG
SD347-R9	CTTCGGGGGTGATCAGAATCCACCAAGTTGTTTCTGTCA GGCCG

Agar-plate and lysate screening of luciferin analogues

Library DNA was transformed into BL21 or T7 Express *lysY E. coli* (New England BioLabs) and plated following the protocol in Jones *et al.*[1] The agar contained luciferin analogues (plated at concentrations ranging from 100–200 μM). Plates were incubated at 37 °C and imaged ~12 h later. Light-emitting colonies were picked and grown for further analyses following the protocol described in Jones *et al.*[1]

Complete analogue/mutant luciferase screen

DNA from functional and sequentially diverse mutants was transformed into *E. coli* BL21. Cells were expanded under antibiotic. Aliquots were stored as glycerol stocks at -80 °C. Luciferin aliquots (10 mM in 100 mM phosphate buffer (pH 7.8) were prepared and stored at -80 °C. Tubes of LB-Kan media (1 mL) were inoculated with each glycerol stock and incubated at 37 °C overnight. The overnight culture was used to inoculate (150 μL) three 5 mL cultures per mutant luciferase. These culture were grown to an OD of ~0.8, induced with 500 μM IPTG for 2 h at 30 °C, then pelleted. Cell pellets were lysed in 600 μL of lysis buffer (50 mM Tris•HCl, 500 mM NaCl, 0.5% (v/v) Tween, 5 mM $MgCl_2$, pH = 7.4). The cell lysate was spread across six wells (90 μL/well) on six different 96-well black plates. Native Fluc was included in each screen as a check on compound integrity. To each well, 10 μL of 10 mM luciferin and 1 mM ATP were added and the plate imaged for 1-60 s. This process was repeated until all 12 compounds were imaged with all 159 luciferase mutants.

***In silico* screens**

Scripts to search for orthogonal sets were written in Python3 and executed on either a MacBook Pro (for testing), or the High Performance Computing Cluster at UC Irvine (https://hpc.oit.uci.edu/). Searches for orthogonal pairs were run on 16 cores. Searches for triplet sets were run on 32 or 64 cores. The Python code and further documentation is freely available online: https://www.chem.uci.edu/~jpresche/resources.html. See the

Supplementary Note for additional information regarding the mathematical evaluation of orthogonality.

Analyzing orthogonality as a function of diversity

Data were generated using Python3 in the Jupyter Notebook environment (code available at https://www.chem.uci.edu/~jpresche/resources.html). For each point on the surface, the algorithm chose 5 random subsets of luciferins and luciferases from the pool of enzyme-substrate data. These subsets were then subjected to the *in silico* screen (see above) and the averages of the top 1,000 orthogonality scores were recorded. All scores were averaged if the total number was less than 1,000. The five subset averages were then further averaged together to give the value of the point.

Mammalian plasmid construction

To express the mutant luciferases in mammalian cells, the luciferase gene was amplified and inserted into pBMN-IRES-GFP[2]. The following primers were used in the amplification:

5'- ataacgcgtatggaagatgccaaaaacattaaga-3' and

5'-gagagggatgcatttattacacggcgatcttgcc-3'

The PCR product was digested with *Nsi*I and *Mlu*I (New England BioLabs) and inserted into the pBMN-IRES-GFP vector with T4 ligase (New England BioLabs). Sequencing analysis was used to confirm the plasmid construct.

Mammalian cell culture

DB7 cells (courtesy of the Contag laboratory, Stanford) were cultured in DMEM (Corning) supplemented with 10% (vol/vol) fetal bovine serum (FBS, Life Technologies), penicillin (100 U/mL), and streptomycin (100 µg/mL). Cells were maintained in a 5% CO_2 water-saturated incubator at 37 °C. To create stable lines expressing mutant luciferases, DB7 cells were transduced with ecotropic retrovirus (Phoenix packaging system) as previously described.[3] Transduced cells were then treated with puromycin (10 µg/mL) and ultiamtely sorted via FACS at the Institute for Immunology Flow Cytometry Core (UCI).

Mammalian cell imaging with luciferase mutants

DB7 cells stably expressing Fluc or mutant luciferases were added to black 96-well plates (1 x 10^5 cells per well). A stock solution of luciferin (5 mM in PBS) was added to each well (500 µM final concentration). Sequential imaging was performed as described in the General bioluminescence imaging section.

In vivo imaging of orthogonal luciferase-luciferin pairs

FVB/NJ mice (The Jackson Laboratory) received subcutaneous dorsal injections of 2 x 10^6 or 6.5 x 10^6 DB7 mutant luciferase expressing cells. After 24 h, animals received an i.p. injection of luciferin (67 mM or 100 mM, 100 µL per mouse). Mice were anesthetized (2% isoflurane) and placed on the warmed (37 °C) IVIS stage for imaging. Bioluminescent photons were quantified for the designated regions of interest. Prior to injecting a second luciferin, mice were imaged for residual bioluminescent signal. Images were acquired every other day over 5 d.

General synthetic methods

All reagents purchased from commercial suppliers were of analytical grade and used without further purification. 4,5-Dichloro-1,2,3-dithiazolium chloride, was prepared as previously reported[4]. Reaction progress was monitored by thin-layer chromatography on EMD 60 F254 plates, visualized with UV light, ceric ammonium molybdate (CAM), chloranil, or $KMnO_4$ stain. Compounds were purified via flash column chromatography using SiliaFlash F60 60 Å, 230-400 mesh silica gel (SiliCycle), unless otherwise stated. HPLC purifications were performed on a Varian ProStar equipped with a 325 Dual Wavelength UV-Vis detector. Semi-preparative runs were performed using an Agilent Prep-C18 Scalar column (9.4 x 150 mm, 5 µm), preparative runs were performed using an Agilent Eclipse XD8-C18 PrepHT column (21.2 x 250 mm 7 µM). Anhydrous solvents were dried by passage over neutral alumina. Reaction vessels were either flame or oven dried prior to use. NMR spectra were acquired with Bruker Advanced spectrometers. All spectra were acquired at 298 K. ^{1}H-NMR spectra were acquired at either 500 or 400 MHz, and ^{13}C-NMR spectra were acquired at 125 MHz. Coupling constants (*J*) are provided in Hz and chemical shifts are reported in ppm relative to either residual non-deuterated NMR solvent, calculated reference, or to a methanol external reference. Low and high-resolution electrospray ionization (ESI) mass spectra were collected at the University of California Irvine Mass Spectrometry Facility.

Synthetic Procedures

4′–BrLuc, 7′–BrLuc, 4′–MeLuc, 7′–MeLuc, 4′–MorphoLuc, 7′–MorphoLuc, 7′–DMAMeLuc and 7′–MorPipLuc were prepared as previously described in Steinhardt *et al*.[5] and Jones *et al.*[1]

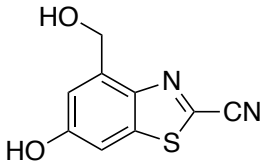

$C_9H_6N_2O_2S$
Mol. Wt. 206.22

6-hydroxy-4-(hydroxymethyl)benzo[d]thiazole-2-carbonitrile (S1). Following the procedure of Kulangiappar *et al.*,[6] 6-acetoxy-4-[bromomethyl]-1,3-benzothiazole-2-carbonitrile[1] (0.150 g, 0.482 mmol), was dissolved in MeCN (10 mL) and stirred at rt in a round bottom flask. Sodium nitrate was dissolved in H_2O (10 mL) and added to the reaction mixture. The flask was flushed with N_2 and then stirred at 80 °C for 22 h. The volatiles were evaporated *in vacuo,* and the resulting aqueous solution was diluted with 1 M $NaHSO_4$ (50 mL) and extracted with EtOAc (3 x 50 mL). The organic layers were combined, washed with brine (1 x 50 mL) and, dried over $MgSO_4$. The solution was filtered and concentrated *in vacuo*. The resulting white solid was carried on without further purification.

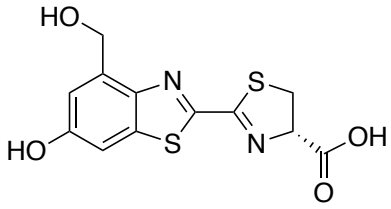

$C_{12}H_{10}N_2O_4S_2$
Mol. Wt. 310.34

(*S*)-2-(6-hydroxy-4-(hydroxymethyl)benzo[*d*]thiazol-2-yl)-4,5-dihydrothiazole-4-carboxylic acid (4´–MeOHLuc).

S1 was dissolved in MeCN (5 mL), added to a scintillation vial, and stirred under N_2. K_2CO_3 (0.067 g, 0.49 mmol) and D-cysteine•HCL•H_2O (0.086 g, 0.49 mmol) were dissolved in H_2O (1 mL) then added to the reaction mixture. When TLC analysis indicated full consumption of starting material, the reaction mixture was concentrated *in vacuo*. The resulting aqueous solution was diluted with H_2O (25 mL), acidified to pH 2, and extracted with EtOAc (5 x 25 mL). The organic layers were combined, dried over $MgSO_4$, filtered, and concentrated *in vacuo* to provide 4´–MeOHLuc, as a dark orange solid (0.087 g, 60%). ^{1}H NMR (400 MHz, D_2O) *δ* 7.14 (d, *J* = 2.2, 1H), 6.99 (d, *J* = 2.2, 1H), 5.20 (dd, *J* = 8.3, *J* = 9.7, 1H), 4.93 (app dd, *J* = 14.0, *J* = 20.8, 2H), 3.81 (app t, *J* = 10.6, 1H), 3.61 (dd, *J* = 8.4, *J* = 11.2, 2H); ^{13}C NMR (125 MHZ, D_2O) *δ* 177.8, 165.9, 157.6, 155.8, 144.0, 137.4, 136.3, 115.0, 105.8, 80.1, 60.4, 36.4. HRMS (ESI$^-$) calcd for $C_{12}H_9O_4N_2S_2$ [M–H]$^-$ = 309.0004, found 308.9994.

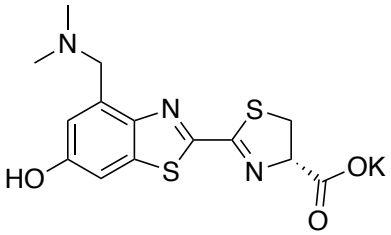

$C_{14}H_{14}KN_3O_3S_2$
Mol. Wt. 375.50

(*S*)-2-(4-((dimethylamino)methyl)-6-hydroxybenzo[*d*]thiazol-2-yl)-4,5-dihydrothiazole-4-carboxylate potassium salt (4´–DMAMeLuc).

To a stirred solution of 6-acetoxy-4-[bromomethyl]-1,3-benzothiazole-2-carbonitrile[1] (0.196 g, 0.630 mmol) in MeCN (2 mL) was added K_2CO_3 (0.261 g, 1.89 mmol) in H_2O (1 mL) and dimethylamine (40 wt. % in H_2O, 0.24 mL, 1.89 mmol). When TLC analysis indicated full consumption of starting material (~30 min), D-cysteine•HCl•H_2O (0.111 g, 0.630 mmol) was added to the reaction mixture. When TLC indicated that the intermediate cyanobenzothiazole was fully consumed, the reaction mixture was concentrated *in vacuo* to yield the potassium salt as a yellow solid (0.13 g, 54%). The product was purified via HPLC (preparative, reversed phase) with the following elution protocol: 100% H_2O for 5 min, followed by a gradient of 0-90% MeOH in H_2O for 15 min. The flow rate was 20 mL/min. ^{1}H NMR (500 MHz, CD_3OD) *δ* 7.24 (s, 1H), 7.04 (s, 1H), 5.16 (t, *J* = 9.3, 1H), 4.04 (app dd, *J* = 13.2, *J* = 20.8, 2H), 3.68 (app p, *J* = 9.1, *J* = 11, 2H) 2.34 (s, 6H); ^{13}C NMR (125 MHz, CD_3OD) *δ* 177.6, 165.8, 159.2, 158.3, 147.7, 139.3, 134.6, 119.1, 106.9, 83.2, 59.6, 45.3, 37.1. HRMS (ESI$^-$) calcd for $C_{13}H_{14}N_3OS_2$ [M–CO_2K]$^-$ = 292.0578, found 292.0573.

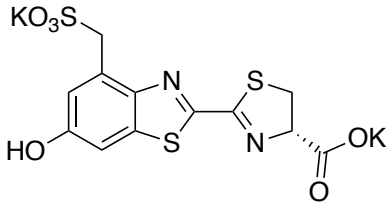

$C_{12}H_8K_2N_2O_6S_3$
Mol. Wt. 450.58

(*S*)-2-(6-hydroxy-4-(sulfonatomethyl)benzo[*d*]thiazol-2-yl)-4,5-dihydrothiazole-4-carboxylate potassium salt (4´–SO_3HLuc).

6-Acetoxy-4-[bromomethyl]-1,3-benzothiazole-2-carbonitrile[1] (0.200 g, 0.643 mmol) was dissolved in acetone (5 mL) and stirred in a round bottom flask. A solution of sodium sulfite (0.243 g, 1.93 mmol) in H_2O (5 mL) was then added. The reaction mixture was then stirred at rt for 24 h. The acetone was removed *via* rotary evaporation. K_2CO_3 (0.090, 0.65 mmol) and D-cysteine•HCl•H_2O (0.114 g, 0.649 mmol) were dissolved in H_2O (1 ml) then added to the reaction mixture. The reaction was stirred at rt for 18 h. Upon completion, the reaction mixture was concentrated *in vacuo* to yield the potassium salt as a yellow solid (0.13 g, 45%). If necessary, the product was purified by HPLC (preparative, reversed phase) with the following elution protocol: 100% H_2O for 5 min, followed by a gradient of 0-90 % MeCN in H_2O for 15 min. The flow rate was 20 mL/min. ^{1}H NMR (500 MHz, D_2O) *δ* 7.29 (d, *J* = 2.4, 1H), 7.11 (d, *J* = 2.4, 1H), 5.22 (dd, *J* = 8.2, *J* = 9.8, 2H), 4.63 (s, 2H), 3.83 (dd, *J* = 9.9, *J* = 11.1, 1H), 3.61 (dd, *J* = 8.2, *J* = 11.1, 1H). ^{13}C NMR (125 MHz, solvent CD_3OD) *δ* 177.6, 165.7,158.5, 158.2, 148.1, 139.0, 131.3, 119.2, 106.7, 83.1, 53.5, 37.3. HRMS (ESI^-) calcd $C_{12}H_9N_2O_6S_3$ $[M–H]^-$ = 372.9623, found 372.9619.

References

1. Jones, K.A. et al. Orthogonal Luciferase-Luciferin Pairs for Bioluminescence Imaging. *J. Am. Chem. Soc.* **139**, 2351-2358 (2017).
2. Liu, H.P. et al. Cancer stem cells from human breast tumors are involved in spontaneous metastases in orthotopic mouse models. *Proc. Natl. Acad. Sci. U.S.A.* **107**, 18115-18120 (2010).
3. Helms, M.W., Prescher, J.A., Cao, Y.A., Schaffert, S. & Contag, C.H. IL-12 enhances efficacy and shortens enrichment time in cytokine-induced killer cell immunotherapy. *Cancer Immunol. Immunother.* **59**, 1325-1334 (2010).
4. McCutcheon, D.C., Porterfield, W.B. & Prescher, J.A. Rapid and scalable assembly of firefly luciferase substrates. *Org. Biomol. Chem.* **13**, 2117-2121 (2015).
5. Steinhardt, R.C. et al. Brominated luciferns are versatile bioluminescent probes. *ChemBioChem* **18**, 96 (2017).
6. Kulangiappar, K., Kulandainathan, M.A. & Raju, T. Conversion of Benzylic Bromides to Benzaldehydes Using Sodium Nitrate As an Oxidant. *Ind. Eng. Chem. Res.* **49**, 6670-6673 (2010).

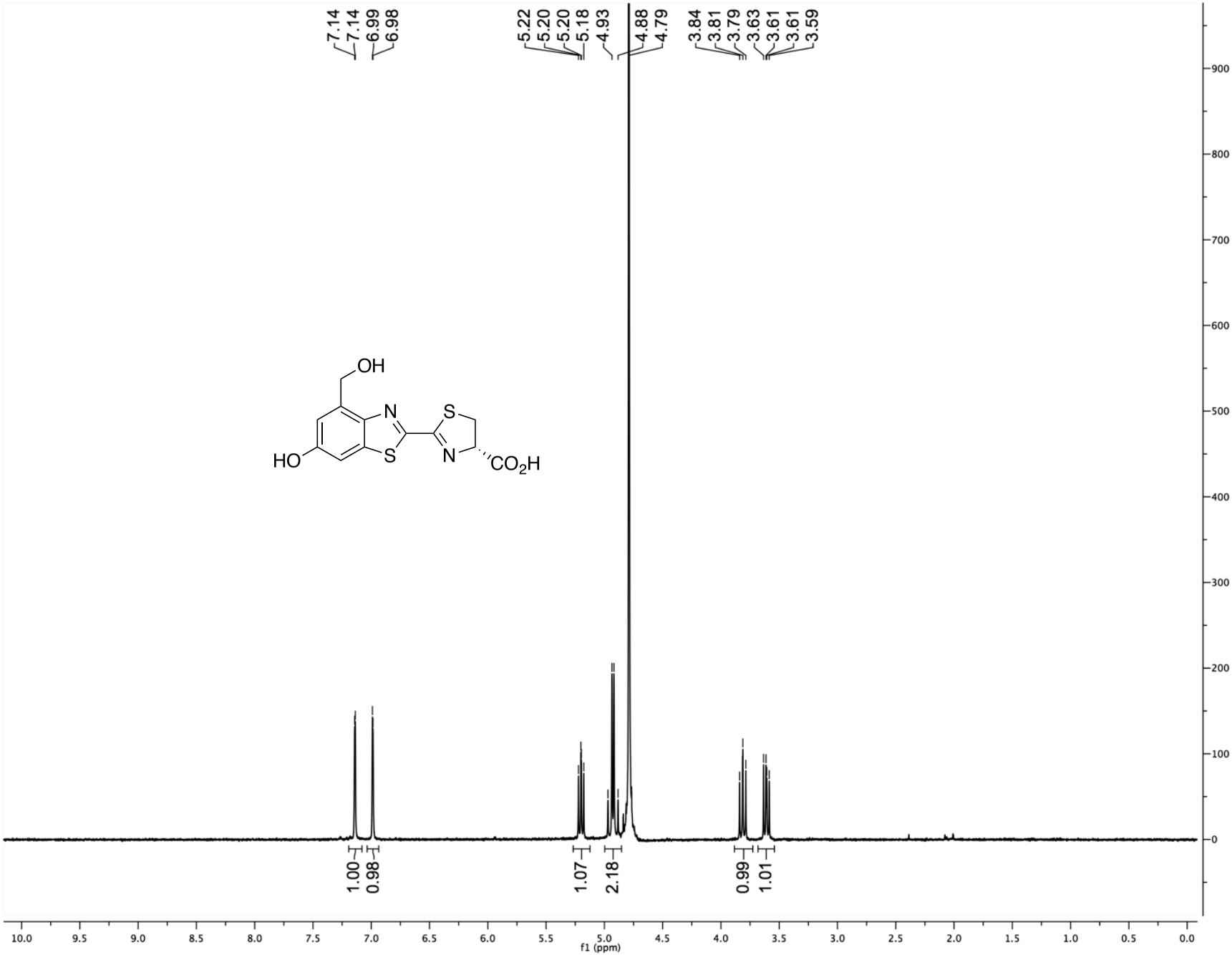
7.14
7.14
6.99
6.98
5.22
5.20
5.20
5.18
4.93
4.88
4.79
3.84
3.81
3.79
3.63
3.61
3.61
3.59
OH
HO
N
S
S
N
CO2H
1.00
0.98
1.07
2.18
0.99
1.01
f1 (ppm)

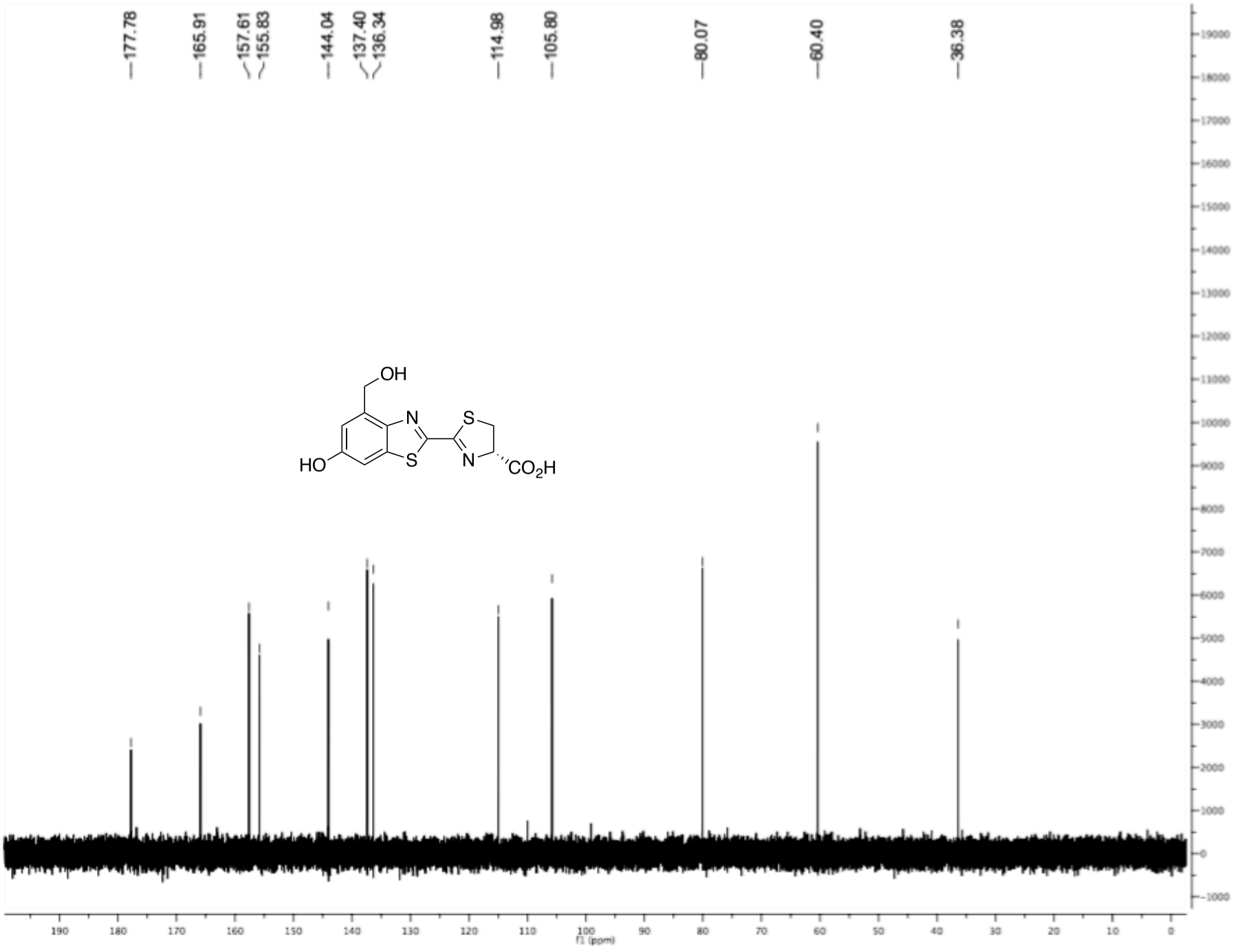
177.78
165.91
157.61
155.83
144.04
137.40
136.34
114.98
105.80
80.07
60.40
36.38
OH
HO
N
S
S
N
CO2H
f1 (ppm)

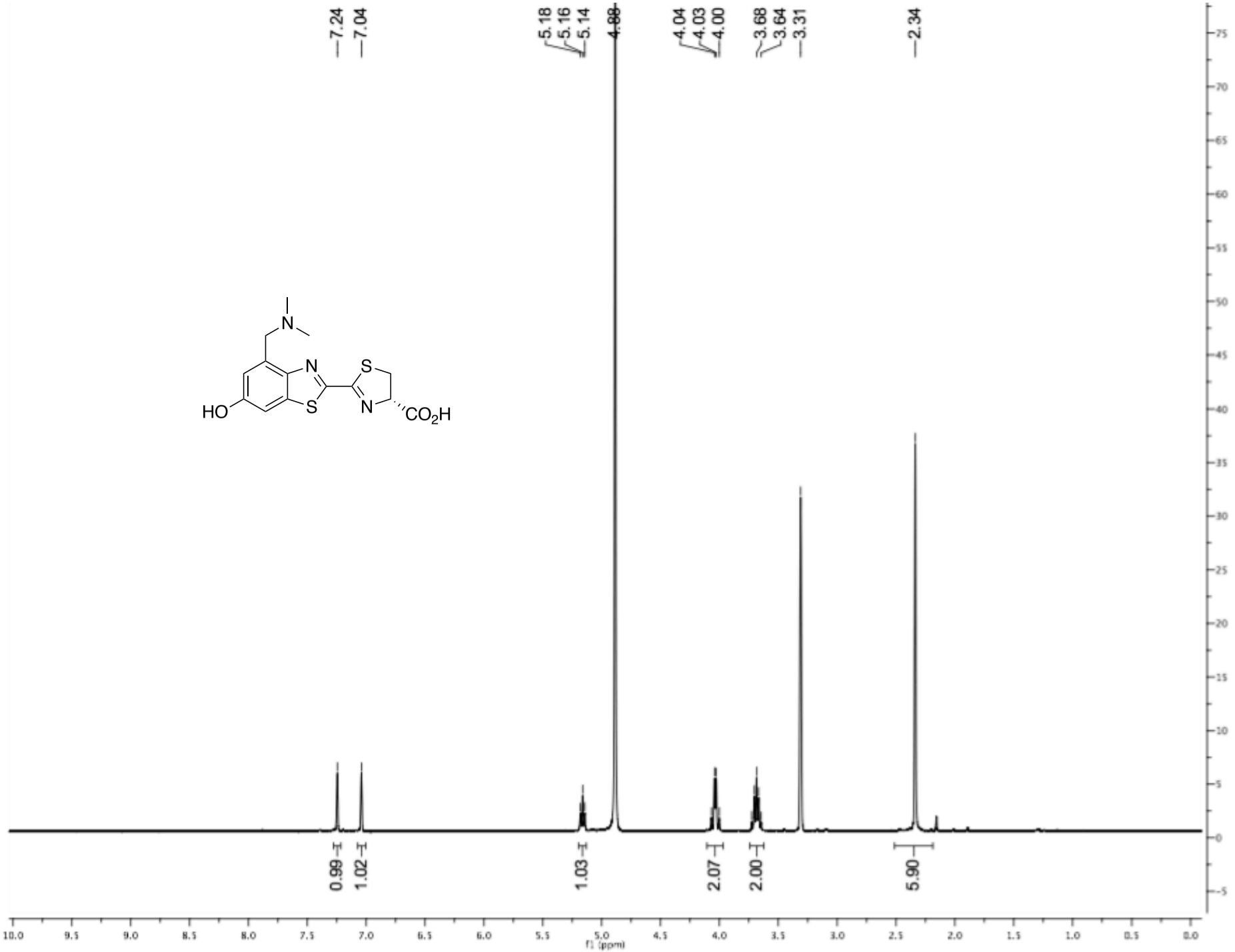
7.24
7.04
5.18
5.16
5.14
4.88
4.04
4.03
4.00
3.68
3.64
3.31
2.34
HO
N
S
N
S
N
CO2H
0.99
1.02
1.03
2.07
2.00
5.90
f1 (ppm)

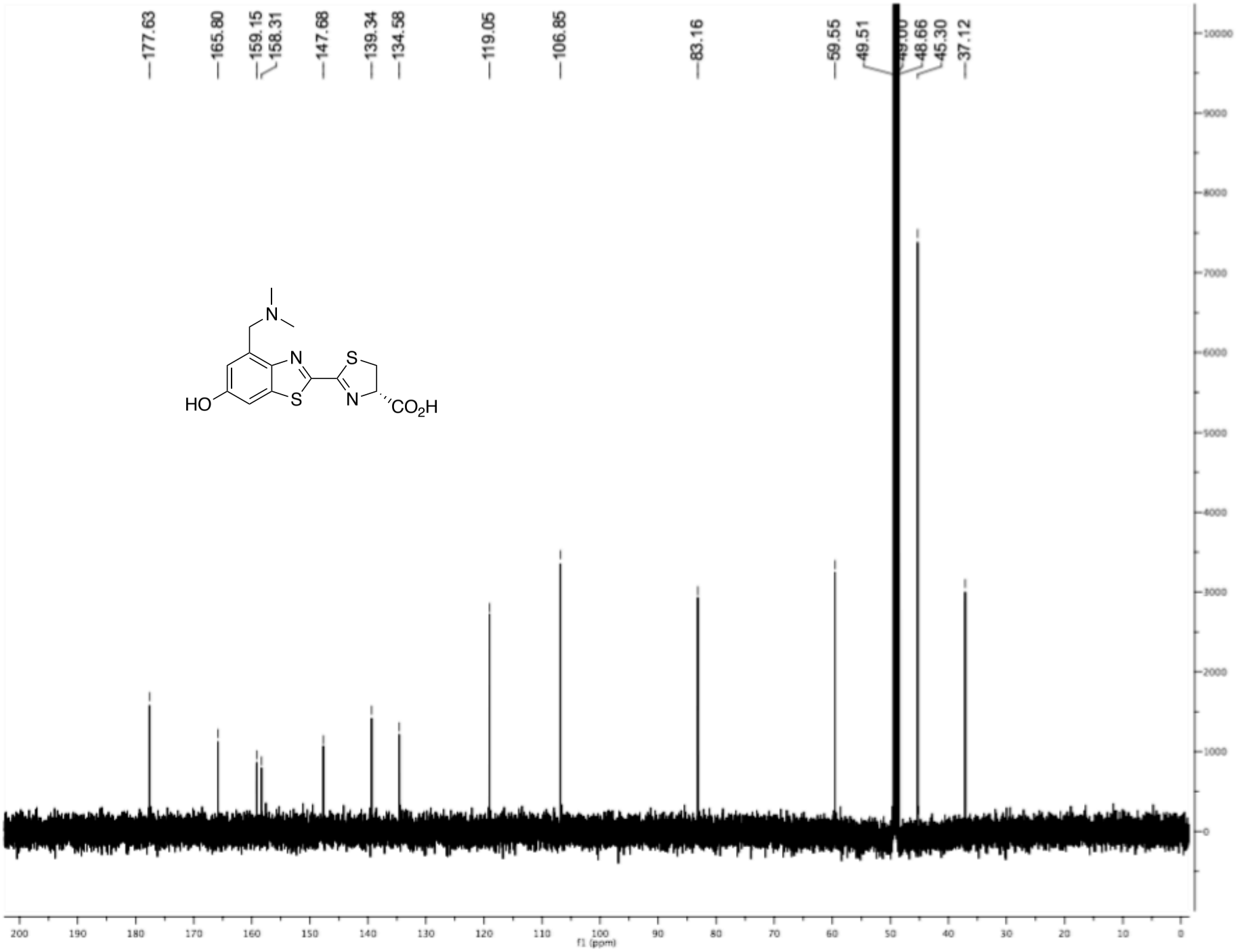
177.63
165.80
159.15
158.31
147.68
139.34
134.58
119.05
106.85
83.16
59.55
49.51
48.66
45.30
37.12
HO
N
S
N
S
N
CO2H
f1 (ppm)

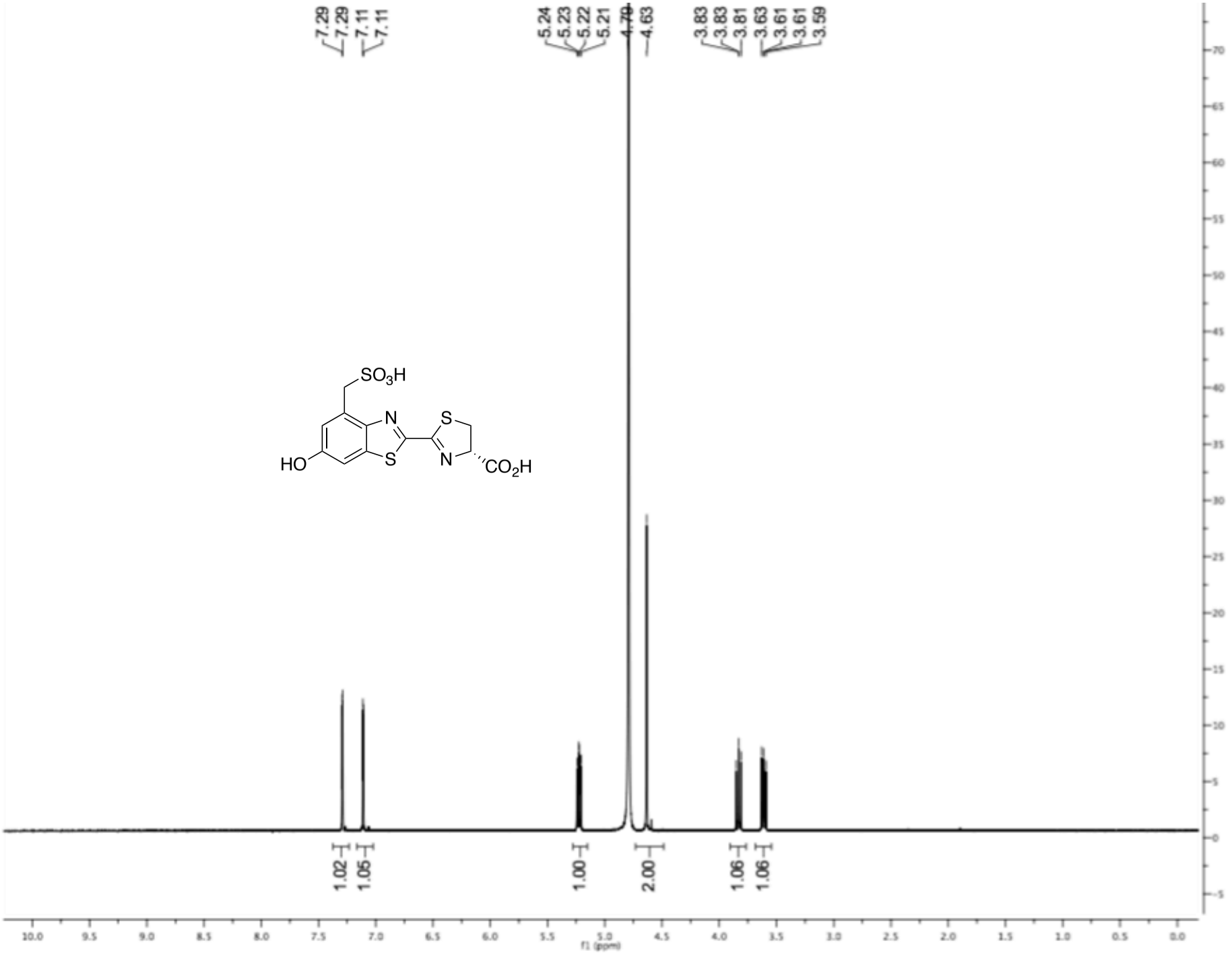
7.29
7.29
7.11
7.11
5.24
5.23
5.22
5.21
4.79
4.63
3.83
3.83
3.81
3.63
3.61
3.61
3.59
SO3H
N
S
HO
S
N
CO2H
1.02
1.05
1.00
2.00
1.06
1.06
f1 (ppm)

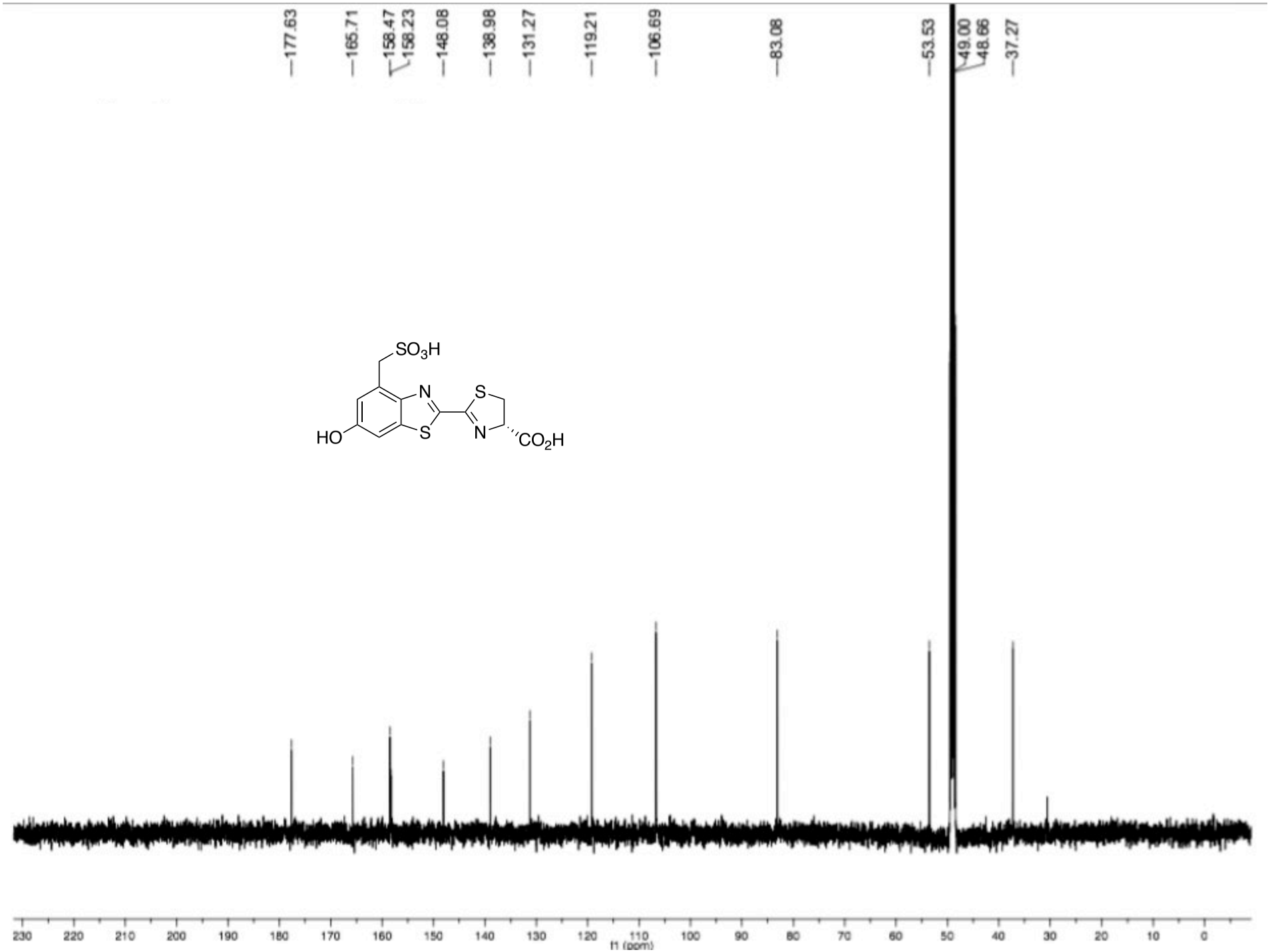
177.63
165.71
158.47
158.23
148.08
138.98
131.27
119.21
106.69
83.08
53.53
49.00
48.66
37.27
SO3H
N
S
HO
S
N
CO2H
230
220
210
200
190
180
170
160
150
140
130
120
110
100
90
80
70
60
50
40
30
20
10
0
f1 (ppm)